Improving the electric field sensing capabilities of the long-period fiber grating coated with a liquid crystal layer

Aleksandra Czapla,[1,*] Wojtek J. Bock,[1] Tomasz R. Woliński,[2] Predrag Mikulic,[1] Edward Nowinowski-Kruszelnicki,[3] and Roman Dąbrowski[3]

[1]*Centre de recherche en photonique, Université du Québec en Outaouais, 101 rue Saint-Jean-Bosco, Gatineau, QC J8X 3X7, Canada*
[2]*Faculty of Physics, Warsaw University of Technology, Koszykowa 75, 00-662 Warsaw, Poland*
[3]*Military Univesity of Technology, 2 Kaliskiego, 00-908 Warsaw, Poland*
[*]*czapla.ale@gmail.com*

Abstract: The hybrid liquid crystal long-period fiber grating structure presented here uses the 1702 liquid crystal as a thin layer on the bare long-period fiber grating. To achieve the highest long-period fiber grating sensitivity to the liquid crystal layer presence, a UV-induced host grating, with a relatively short period of 226.8 μm, was chosen. This design makes it possible to couple light from the propagating core mode to a cladding mode at a wavelength near the phase-matching turning point. This phenomenon is exploited here for the first time to measure the thermal and electric field responses of the liquid crystal long-period fiber grating structure. All experimental results achieved in this work are supported by theoretical analysis.

OCIS codes: (060.2370) Fiber optics sensors; (050.1950) Diffraction gratings; (060.2300) Fiber measurements.

References and links

1. G. Rego, "A review of refractometric sensors based on long period fibre gratings," Sci. World J. **2013**, 913418 (2013).
2. E. Brzozowska, M. Śmietana, M. Koba, S. Górska, K. Pawlik, A. Gamian, and W. J. Bock, "Recognition of bacterial lipopolysaccharide using bacteriophage-adhesin-coated long-period gratings," Biosens. Bioelectron. **67**, 93–99 (2015).
3. M. Konstantaki, A. Klini, D. Anglos, and S. Pissadakis, "An ethanol vapor detection probe based on a ZnO nanorod coated optical fiber long period grating," Opt. Express **20**(8), 8472–8484 (2012).
4. X. Shu, L. Zhang, and I. Bennion, "Sensitivity characteristics of long-period fiber gratings," J. Lightwave Technol. **20**(2), 255–266 (2002).
5. I. Del Villar, "Ultrahigh-sensitivity sensors based on thin-film coated long period gratings with reduced diameter, in transition mode and near the dispersion turning point," Opt. Express **23**(7), 8389–8398 (2015).
6. S. M. Tripathi, W. J. Bock, A. Kumar, and P. Mikulic, "Temperature insensitive high-precision refractive-index sensor using two concatenated dual-resonance long-period gratings," Opt. Lett. **38**(10), 1666–1668 (2013).
7. M. Smietana, W. J. Bock, P. Mikulic, and J. Chen, "Tuned pressure sensitivity of dual resonant long-period gratings written in boron co-doped optical fiber," J. Lightwave Technol. **30**(8), 1080–1084 (2012).
8. O. Frazão, G. Rego, M. Lima, A. Teixeira, F. M. Araújo, P. André, J. F. Rocha, and H. M. Salgado, "EDFA gain flattening using long-period fiber gratings based on the electric arc technique," in *Proc. London Communications Symposium 2001* (2001), pp. 55–57.
9. X. J. Gu, "Wavelength-division multiplexing isolation fiber filter and light source using cascaded long-period fiber gratings," Opt. Lett. **23**(7), 509–510 (1998).
10. T. A. Eftimov, W. J. Bock, P. Mikulic, and J. Chen, "Müller–Stokes analysis of long-period gratings Part II: Randomly birefringent LPGs," J. Lightwave Technol. **27**(17), 3759–3764 (2009).
11. J. L. Arce-Diego, D. Pereda-Cubian, and M. A. Muriel, "Polarization effects in short- and long-period fiber gratings: a generalized approach," J. Opt. A, Pure Appl. Opt. **6**(3), S45–S51 (2004).
12. I. C. Khoo and S. T. Wu, "Optics and Nonlinear Optics of Liquid Crystals" (World Scientific Publ., 1997).
13. J. Li and S.-T. Wu, "Extended Cauchy equations for the refractive indices of liquid crystals," J. Appl. Phys. **95**(3), 896–901 (2004).

#255891 Received 16 Dec 2015; revised 18 Feb 2016; accepted 19 Feb 2016; published 4 Mar 2016

14. O. Duhem, J. F. Henniont, M. Warenghem, M. Douay, and L. Rivoallan, "Long-period fiber gratings modulation by liquid crystal cladding," in *Proc. 6th IEEE Conf. on Telecommunications* (1998), pp. 195–196.
15. S. Yin, K.-W. Chung, and X. Zhu, "A novel all-optic tunable long-period grating using a unique double-cladding layer," Opt. Commun. **196**(1-6), 181–186 (2001).
16. H. R. Kim, Y. Kim, Y. Jeong, S. Baek, Y. W. Lee, B. Lee, and S. D. Lee, "Suppression of the cladding mode interference in cascade long-period fiber gratings with liquid crystal cladding," Mol. Cryst. Liq. Cryst. (Phila. Pa.) **413**, 399–406 (2004).
17. A. Czapla, T. R. Woliński, W. J. Bock, E. Nowinowski-Kruszelnicki, R. Dąbrowski, and J. Wójcik, "Long-Period Fiber Gratings with Low-Birefringence Liquid Crystal," Mol. Cryst. Liq. Cryst. (Phila. Pa.) **502**(1), 65–76 (2009).
18. H. Luo, X. Li, S. Li, and J. Chen, "Analysis of temperature-dependent mode transition in nanosized liquid crystal layer-coated long period gratings," Appl. Opt. **48**(25), F95–F100 (2009).
19. A. Czapla, W. J. Bock, T. R. Woliński, R. Dabrowski, and E. Nowinowski-Kruszelnicki, "Tuning Cladding-Mode Propagation Mechanisms in Liquid Crystal Long-Period Fiber Gratings," J. Lightwave Technol. **30**(8), 1201–1207 (2012).
20. A. Czapla, W. J. Bock, and T. R. Wolinski, "Designing sensing properties of the long-period fiber grating coated with the liquid crystal layers," Proc. SPIE **8421**, 84215H (2012).
21. J. G. Delly, "The Michel-Lévy interference color chart. The microscopist's magical color key," (Modern Microscopy, 2003), http://www.modernmicroscopy.com/main.asp?article=15
22. M. S. Chychłowski, S. Ertman, E. Nowinowski-Kruszelnicki, and T. R. Woliński, "Escaped radial and planar liquid crystal orientation inside capillaries," Mol. Cryst. Liq. Cryst. (Phila. Pa.) **553**(1), 127–132 (2012).
23. M. S. Chychłowskia, O. Yaroshchuk, R. Kravchuk, and T. R. Woliński, "Liquid crystal alignment in cylindrical microcapillaries," Opto-Electron. Rev. **20**, 47–52 (2012).
24. D. Budaszewski, A. K. Srivastava, A. M. W. Tam, T. R. Woliński, V. G. Chigrinov, and H.-S. Kwok, "Photo-aligned ferroelectric liquid crystals in microchannels," Opt. Lett. **39**(16), 4679–4682 (2014).
25. S. V. Shiyanovskii, O. D. Lavrentovich, T. Schneider, T. Ishikawa, I. I. Smalyukh, C. J. Woolverton, G. D. Niehaus, and K. J. Doane, "Lyotropic chromonic liquid crystals for biological sensing applications," Mol. Cryst. Liq. Cryst. **434**(1), 259587 (2005).
26. K. Iwabata, U. Sugai, Y. Seki, H. Furue, and K. Sakaguchi, "Applications of Biomaterials to Liquid Crystals," Molecules **18**(4), 4703–4717 (2013).
27. S. Ertman, K. Bednarska, A. Czapla, and T. R. Wolinski, "Photonic liquid crystal fibers tuning by four electrode system produced with 3D printing technology," Proc. SPIE **9634**, 96345F (2015).

1. Introduction

Optical fibers with micro-periodic structures have generated great interest in the scientific community due to the new possibilities they offer for light guiding and control that have not been obtainable with conventional optical fibers. Such structural features are also a key element in novel optical fiber sensing devices. One of the most mature classes of this kind of fiber device comprises long-period fiber gratings (LPFGs). Within a relatively short time it became obvious that LPFGs could be successfully incorporated into an optical communications network or into a fiber-optic sensing system since they provide a mechanism for producing a wavelength-dependent attenuation in the transmission spectrum which can be controlled by external effects. The main relation describing wavelength-dependent coupling from the guided core mode (LP_{01}) to the m cladding mode (LP_{0m}) is expressed as follows: $\lambda_{res,m} = \Lambda\left(n_{co}^{eff} - n_{cl,m}^{eff}\right)$, where n_{co}^{eff}, $n_{cl,m}^{eff}$, and Λ stand for the effective refractive index (RI) of the core mode, the effective RI of the *m*th cladding mode and the period of the LPFG, respectively. One of the most distinctive properties of LPFGs is that they are highly sensitive to the surrounding media. Consequently, they can be used as refractometers or for chemical substance detection in the environment [1]. Furthermore, it was presented that if an overlay is deposited on the LPFG cladding, its refractive index (RI) will modify the coupling of modes. If the overlay material selected is sensitive to a specific parameter, highly sensitive and specific devices will be obtained, including e.g. a number of chemosensors and biosensors [2,3]. It is also important noting that, up to a certain point, an increase in the LPFG sensitivity follows an increase in the order of the coupled cladding mode. Shu et al. found that when the grating period of the LPFG is short enough, the optical power coupling to the higher-order cladding modes leads to a phenomenon of dual resonance [4]. At dual resonance, the same cladding mode is excited at two distinct wavelengths, both of them shifting in opposite directions from each other with the variation of a number of parameters [5]. This feature is of

#255891 Received 16 Dec 2015; revised 18 Feb 2016; accepted 19 Feb 2016; published 4 Mar 2016

great interest in sensing applications because it nearly doubles the sensitivity of the LPFG-based sensor. The closer the grating period to the turnaround point (TAP), the greater the sensitivity. Several applications of LPFGs operating at TAP for temperature, strain, pressure and RI sensing have been shown [6,7]. LPFGs could also found a variety of applications in optical communications as gain-flattening filters for erbium-doped fiber amplifiers (EDFAs) [8], as wavelength division multiplexing (WDM) systems [9], and as wavelength-selective optical fiber polarizer components [10,11]. Compared to other optical devices, LPFGs have a number of unique advantages such as low-level back reflection, compact construction, low insertion losses, resistance to harsh environments, immunity to electromagnetic interference and often greater sensitivity than conventional sensors.

LPFGs combined with liquid crystals (LCs) have been seen as promising structures for creating a new platform for tunable fiber devices. LCs are self-organized anisotropic materials that exhibit high electro- and thermo-optic effects associated with their birefringence, their dielectric anisotropy and the thermal dependence of their RIs [12,13]. Merging the unique properties of LCs with LPFGs in this way has extended the sensing capabilities of the LPFG and created a new class of photonic components, known as LC-LPFGs. Experiments carried out in the last decade have shown that LC-LPFGs can realistically contribute to the development of new photonic devices. One of the first examples of LPFG tuning by using LC was demonstrated by Duhem et al. [14]. They proposed a modulation of the attenuation band intensity based on the electrical switching of a nematic liquid crystal (NLC) around a photo-induced LPFG. Yin et al. presented a device based on an ultrathin LPFG etched by hydrofluoric acid (HF), which was surrounded by a dye-doped NLC for tuning the resonant wavelength [15]. The NLC in the outer cladding of the proposed LC-LPFG was switched by a polarized Ar^+ laser, thus providing an all-optical tuning of the attenuation band (in the order of a few nm) in the LPFG transmission spectrum. Furthermore, a cascade structure of LPFGs with LC as the surrounding medium was proposed by H-R Kim et al. [16] for arbitrary loss filters that could compensate a non-uniform optical gain in an EDFA. The results show that the interference effects in cascaded LPFGs can be suppressed using an extended LC cladding and the amount of the reflection can be controlled by an electric field across the LC cladding. Also noteworthy are the results presented in [17] where LPFGs, based on the SMF-28 and photonic crystal fibers (PCF), surrounded by a low-birefringence (LB) 1550 LC mixture were thermally and electrically tuned. In this work, a special glass capillary with five holes was used, where metal wires were placed in four holes (serving as electrodes) while the LPFG was introduced in the central hole and then filled with the LC. Next, the idea of a coated LPFG with a thin LC layer (in the order of 1 μm) was brought forward by Luo et al. [18]. The host LPFG used in this research was fabricated by CO_2 laser irradiation, and medium-birefringence (MB) LC was employed as a LC layer. The experimental results along with the theoretical analysis presented there showed that efficient thermal tuning can be achieved for such a LC-LPFG design (up to 80 nm). However, the authors of this publication did not include the thermal response of the host fiber in their theoretical model (a factor which can significantly contribute to LC-LPFG thermal sensitivity). Later, in [19] the electric and thermal tuning of the UV-induced LPFG combined with low-birefringence (LB) LC mixtures was presented. In this work, two different methods were used in order to obtain an LC coating on the LPFG: placing the LPFG inside a capillary and filling it with LC, or directly coating the bare LPFG with a thin LC layer. It was shown that the LPFG, when enhanced with an external LB LC layer, exhibits two different temperature sensitivities, which depend on the temperature range of operation (corresponding with a nematic and an isotropic LC phases). Moreover, the "switching" functionality of this LC-LPFG around the LC clearing temperature T_c was observed (useful, for example, in warning systems). The electric induced shift of the attenuation band (up to 11 nm) was achieved as well for the presented there LC-LPFG design. Finally, in [20] it was demonstrated that a temperature compensation effect could be obtained for an LPFG with an 1800b LB LC. In the transmission spectrum of this LC-LPFG structure,

#255891 Received 16 Dec 2015; revised 18 Feb 2016; accepted 19 Feb 2016; published 4 Mar 2016

the thermal sensitivity of the attenuation band in terms of band depth and its resonant wavelength was found to be almost nine times lower than the sensitivity of the band for LPFGs in air.

In this paper, the use of the hybrid LC-LPFG structure takes advantage of the 1702 medium-birefringence and high positive dielectric anisotropy LC serving as a thin layer on a LPFG. To explore the benefits of the host LPFG, we chose the relatively short period of 226.8 μm, offering the possibility of operating near the TAP. To the best of our knowledge, the work reported here exploits this phenomenon for the first time as a way of measuring the LC-LPFG structure's thermal and electric field responses. As far as the thermal sensitivity of this LC-LPFG is concerned, we will show that the generation of dual resonant bands occurs in its transmission spectrum with an increase in temperature. Thanks to the electro-optical properties of the LC material, the LC-LPFG demonstrates electric sensitivity in addition to the sensitivities of the grating itself. We will further show that the electric switching capabilities of the LC-LPFG can be significantly improved by a proper choice of the operating temperature range. All results of the experiments in this work investigating the concept of an LPGF coated with a high-RI thin layer of LC are supported by theoretical analysis, based on a model developed with Optigrating v.4.2 software.

2. Materials and experimental process

To carry out the experiments, we fabricated an LPFG using an Eximer laser (*PulseMaster GSI Lumonics* emitting at a wavelength of 248 nm). As a host fiber, a boron co-doped photosensitive fiber (*Fibercore* PS1250/1500) was chosen. The details of the LPFG fabrication procedure can be found in [8]. The grating period was 226.8 μm. This short period allowed us to achieve a resonance wavelength close to the TAP in the presence of air as a surrounding medium (see Fig. 1 where the measured and simulated LPFG thermal response is presented).

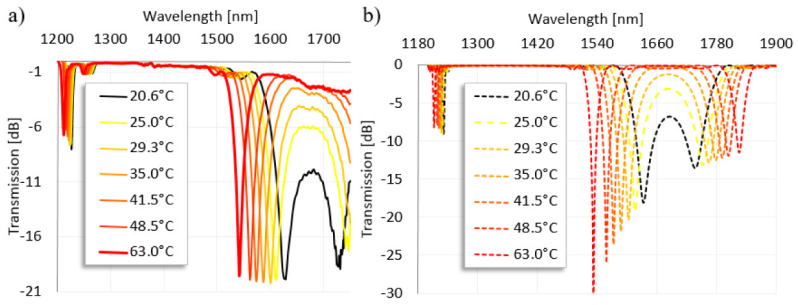

Fig. 1. Measured and simulated thermal response of the host LPFG (based on PS1250/1500 fiber, with period and length of 226.8 μm and 3.5 cm, respectively).

As an external layer for the LPFG, we used a prototype 1702 LC (synthesized at Military University of Technology, Warsaw, Poland). This LC is characterized by the medium birefringence equal to 0.17. The temperature dependencies of its RIs are presented in Fig. 2b (note that both the ordinary n_o and extraordinary n_e RIs are higher than the RI of silica glass, n_{SiO_2}). Clearing temperature T_c for this LC is 86°C, melting point < –12°C. The 1702 LC is also characterized by a high positive dielectric anisotropy $\Delta\varepsilon$ (~48.4 at 25°C), enabling a relatively easy molecular reorientation by using an external E-field. The 1702 LC temperature dependence of electric permittivity constants is presented in Fig. 2(b). In order to create our LC-LPFG, a thin LC layer was formed on the bare LPFG. The surface tension of the LC facilitates the creation of a uniform coat on the LPFG, resulting in a thin (micron scale) overlay. It has to be emphasized here that LC alignment is of prime importance since it has a significant effect on the LC RI value. The LC molecule orientation on the bare LPFG is

#255891 Received 16 Dec 2015; revised 18 Feb 2016; accepted 19 Feb 2016; published 4 Mar 2016

mainly determined by the anchoring conditions. In order to provide a better alignment of the LC, the LPFGs were first rubbed several times along the fiber axis with a cotton swab. As a result, the LC molecules tended to align along the fiber axis and it is reasonable to assume that satisfactory LC planar alignment was then present on the LPFG. Consequently, the effective RI of the LC layer can be approximated by a value close to the LC n_o . The presence of the LC layer on the surface of the LPFG was confirmed when the sample was placed between two polarizers (in the same way as for the LC-LPFG presented in [18], where the picture of the LPFG with the LC layer highlighted is presented). Then, referring to the Michel-Levy interference chart [21], we were able to estimate the thickness of the 1702 LC layer to be of the μm order. Thickness of the LC layers could be more precisely determined through theoretical analysis (presented in the next section) and it was assessed to be of 2.1 μm.

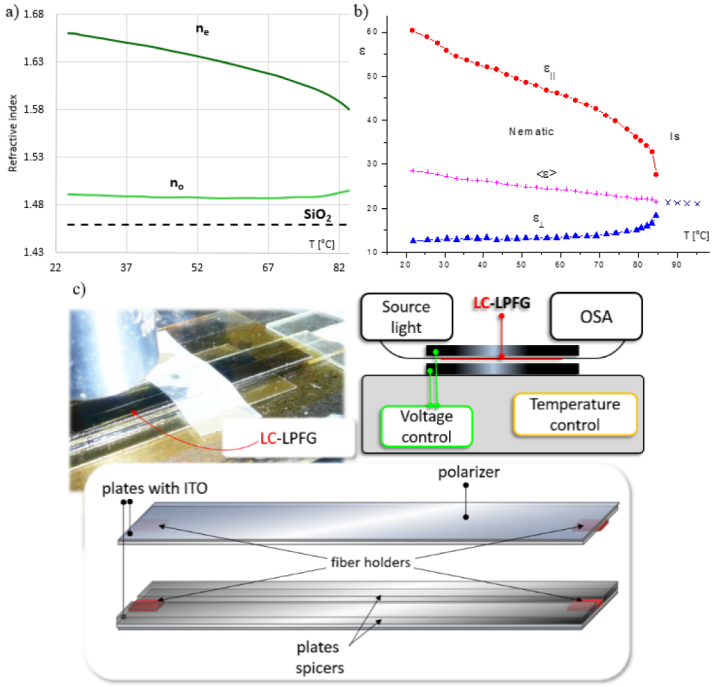

Fig. 2. (a) The 1702 LC thermal dependencies of ordinary n_o, extraordinary n_e, as well silica glass n_{cl} refractive indices measured at wavelength of 589 nm. (b) The 1702 LC temperature dependence of electric permittivity constants. (c) Experimental setup with picture and schema of the LC-LPFG housing unit

The LC-LPFGs were next tested under the influence of temperature by placing them on the hot side of a Peltier module, keeping the temperature within the 10°C –100°C range. In order to apply an external E-field to the sample, the LC-LPFG was placed in a specially designed housing unit. Two plates with ITO served as electrodes, which were separated from each other by 135 μm. Electrical control was achieved within a range between 0 V/μm to 4 V/μm. It is also worth noting that this housing unit prevents LC-LPFG cross-sensitivity to physical parameters such as stress and bending, as well providing temperature stabilization The transmission spectra of the sample were investigated with input light launched from an Agilent 83437 broadband light source and the output signal was analyzed by an Optical Spectrum Analyzer (OSA).

#255891 Received 16 Dec 2015; revised 18 Feb 2016; accepted 19 Feb 2016; published 4 Mar 2016

3. Theoretical analysis of the LC-LPFG

3.1 LC-LPFG model

Optical simulations of the LC-LPFG were performed using OptiGrating v.4.2 software by Optiwave. The study LC-LPFG model is composed of four layers (the fiber core, the fiber cladding, the LC layer surrounded by a fourth layer of air). The grating period is determined during the fabrication process, and is set at 226.8 μm. The grating length is fixed at 3.5 cm. The fiber model is based on the manufacturer's datasheets for the fiber used in the experimental work (boron co-doped photosensitive Fibercore PS1250/1500 fiber). The exact parameters used in the LPFG model are summarized in Table 1.

Table 1. Specification of the LPFG model

LPFG parameters		Fiber parameters	
Grating length [μm]	35000	n_{co}	1.449326
Grating period [μm]	226.8	n_{cl}	1.44403
		r_{co}	3.97
Index modulation within the core	2×10^{-4}	r_{cl}	59.3

The LC thermal characteristic applied to the LC-LPFG model is presented in Fig. 3 (dash line). We determined the dispersion properties of the LC by using the extended Cauchy formula [12]. Unfortunately, the precision of the LC layer thickness measurement under the experimental work was limited (we were able to determine its value to be a few micrometers). However, by fitting the LC-LPFG transmission spectra as measured in air versus temperature and/or electric field with data from the simulation, we arrived at an estimated thickness of 2.1 μm.

3.2 Modeling the LC-LPFG thermal response

In order to investigate the thermal impact on the spectral properties of the LC-LPFG, three effects have to be considered: the LPFG sensitivity to temperature (described for example in [18]), the LPFG sensitivity to the presence of the LC layer, and finally, the LC layer thermal characteristic. In order to develop our LC-LPFG model which takes all these effects into account, we performed computer simulations in two steps. First, we calculated new values for the RIs of the core $n_{co,T}$ and cladding $n_{cl,T}$ corresponding with certain values of the ambient temperature T as follows:

$$n_{co,T} = n_{co,T_{REF}} + (T - T_{REF}) n_{co,T_{REF}} \xi_{co} \quad (1)$$

$$n_{cl,T} = n_{cl,T_{REF}} + (T - T_{REF}) n_{cl,T_{REF}} \xi_{cl} \quad (2)$$

, where T_{REF} (set in the simulation to be 25°C) is a reference temperature; $n_{co,T_{REF}}$ and $n_{cl,T_{REF}}$ are RIs of the core and cladding at T_{REF}; ξ_{co} and ξ_{cl} are thermo-optic coefficients for the core and cladding (set in the simulation to be equal to 6.9×10^{-6} 1/°C and to 8.3×10^{-6} 1/°C, respectively). Secondly, using the OptiGrating software, we simulated the LC-LPFG transmission spectra according to these new core $n_{co,T}$ and cladding $n_{cl,T}$ values corresponding to certain ambient temperatures. At the same time, we selected the RI values of the LC layer appropriate to each of the temperature values given by the LC thermal characteristic in Fig. 4 (dash line). The simulations allowed us to theoretically compare the thermal sensitivity of the LPFG in air and the LPFG with a 1702 LC layer. Figure 3 shows the thermal response of the dual resonant band calculated for these two cases. The spectral range was selected arbitrarily in order to clearly show the variations of the attenuation band close to the TAP. From these results it is clear that the initial position of the dual resonant band is

#255891 Received 16 Dec 2015; revised 18 Feb 2016; accepted 19 Feb 2016; published 4 Mar 2016

different after the LPFG is coated with a thin 1702 LC layer: the attenuation band starts to appear at 1687 nm for the LPFG in air and at 1648 nm for the LC layer. We also found that the observed attenuation bands result from the coupling of different order modes. Specifically, in the case of the LPFG in air the attenuation band appears when the $LP_{0,10}$ mode is engaged, while in the case of the LC-LPFG, the dual resonant band is associated with the $LP_{0,11}$ mode. However, the thermal tuning behavior of these attenuation band types is similar whether the LPFG is in air or coated with the LC layer – the single broader resonance splits into the two resonance wavelengths around TAP when temperature increases. It can therefore be concluded that by a proper choice of operating temperature, the RI of the LC layer may be adjusted to a certain extent. This feature is later explored in this work in order to enrich the LC-LPFG electric properties.

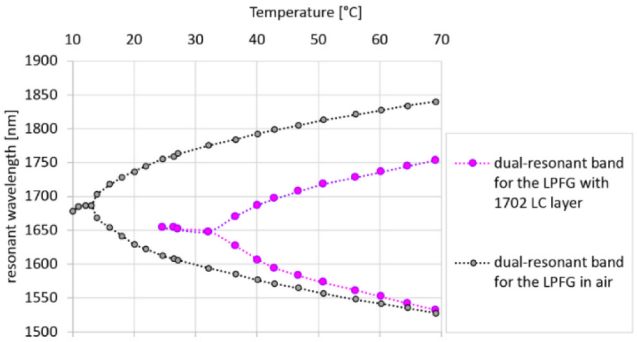

Fig. 3. Simulated thermal sensitivities for the LPFG in air and coated with the 1702 LC layer. The spectral range has been selected arbitrarily in order to show the variations of the attenuation band close to the TAP.

3.3.Modeling the LC-LPFG electric response for different operating temperatures

In order to study the electric response of the LC-LPFG, the RIs of the LC layer with and without E-field has to be defined well. We also need to keep in mind that the ambient temperature can change the LC-LPFG sensitivity to the E-field. Figure 4 shows the thermal characteristic of the n_o and n_e for the LC used in the experimental work 1702, which was estimated for the wavelength of 1550 nm. In the same Figure the RI values (for the case of with and without E-field) versus temperature applied in the simulation are presented. The differences between LC RI values gives by the 1702 LC thermal characteristic and used in calculations stem from two main reasons. First, in the LC-LPFG model it is assumed that the orientation of LC molecules on the bare LPFG is perfect. Obviously, this situation never occurs in reality. The actual alignment will mainly affect the n_o and n_e values. The less perfect the alignment, the higher the value of the n_o and the lower the value of the n_e will be. This effect was included in the model by slightly adjusting the RI of the LC layer when the simulated and measured spectra were compared. Second, when the LC-LPFG electric properties were experimentally studied, a setup with two parallel electrodes was used. As a result, the E-field is perpendicular to the LPFG axis. In practice this means that the anisotropy in the LC layer may be induced. In the LC-LPFG model studied here, an isotropic RI distribution within the LC layer was assumed, although such an assumption might introduce an error into the calculations. However, this assumption makes it easier to understand the effect of the E-field on an LC-LPFG, and the model still adequately accounts for the experimental results. For now, in order to include the LC layer anisotropy effect, we estimated the value of the RI of the LC layer in the presence of an E-field when comparing the simulated electric responses of the LC-LPFGs to those measured in the experiment. We then used the following fitting procedure: first, we assessed the LC layer thickness value by

#255891 Received 16 Dec 2015; revised 18 Feb 2016; accepted 19 Feb 2016; published 4 Mar 2016

matching the simulation results to the experimentally measured LC-LPFG transmission spectrum without an E-field (the LC layer RI corresponds in this case with the n_o value of the LC); secondly, we found the RI of the LC layer in the on-voltage state by matching the simulation results to the experimentally measured LC-LPFG transmission spectrum when the E-field was applied to the sample.

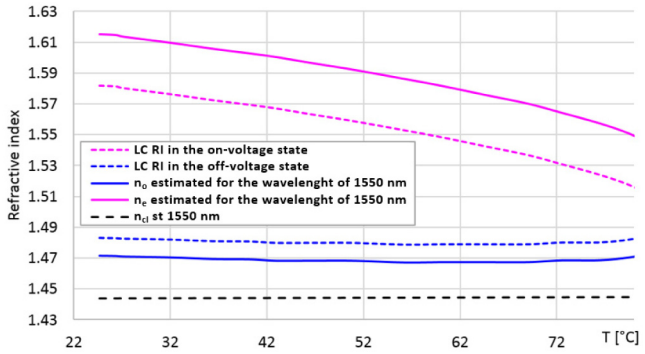

Fig. 4. Thermal characteristics of the 1702 LC estimated for the wavelength of 1550 nm (solid line) and applied to the simulation (dash line).

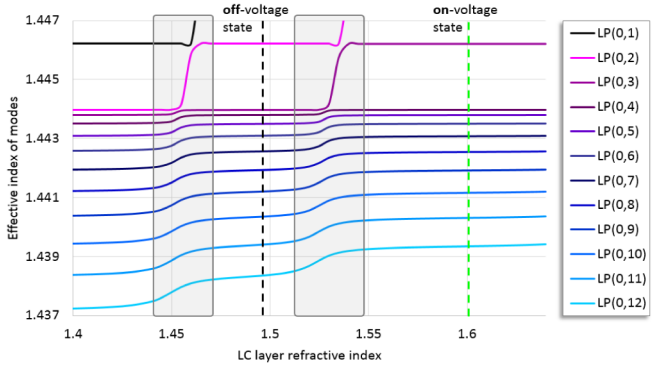

Fig. 5. Mode structure plot versus LC layer refractive index calculated for the wavelength of 1550 nm.

Our simulations showed that the difference between estimated 1702 LC refractive indices, without and with E-field, is sufficient to obtained the transformation of the lowest-order cladding mode (higher effective RI) into a guided mode within the LC layer. The immediate consequence of this change is a reorganization of the other cladding modes (the LC RI interval where this transition occurs is highlighted in Fig. 5 by the grey rectangle). As a result, the LC-LPFG is able to operate between two states of the attenuation bands, namely the off-voltage state, corresponding with the planar LC layer orientation on the bare LPFG (designated in Fig. 4 by the blue dash line), and the on-voltage state, corresponding with the orthogonal LC layer orientation on the bare LPFG (designated in Fig. 4 by the pink dash line).

4. Experimental results and discussion

Thanks to the electro-optical properties of the 1702 LC materials, the LC-LPFG demonstrated electric sensitivity in addition to the sensitivities of the grating itself. In [19] we showed that this same combination of LPFG and LC was found to have a fast and repeatable switching ability within the attenuation band in its transmission spectrum (up to almost 8 nm) in the spectral range from 1185 nm to 1240 nm. However, we were unable to achieve this effect for the attenuation band close to TAP: after the LPFG was coated with a LC layer, the attenuation

#255891 Received 16 Dec 2015; revised 18 Feb 2016; accepted 19 Feb 2016; published 4 Mar 2016

band vanished from the transmission spectrum. Here, we demonstrate that the electric switching capabilities for the same LPFG and LC combination can be significantly improved through strategic choice of the operating temperature range.

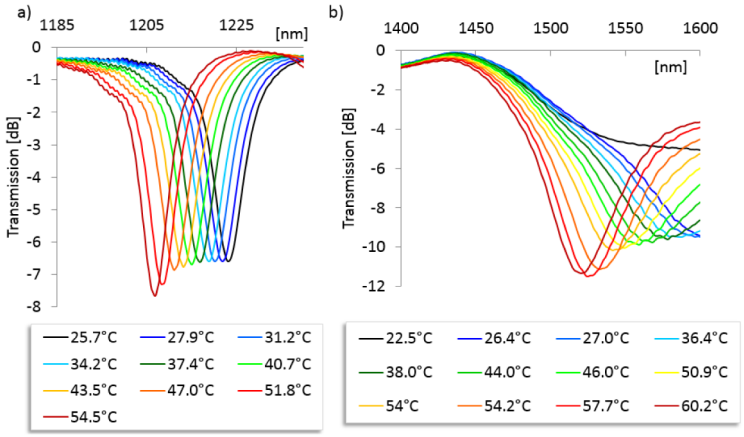

Fig. 6. Measured transmission spectra versus temperature for the LPFG coated with the 1702 LC layer

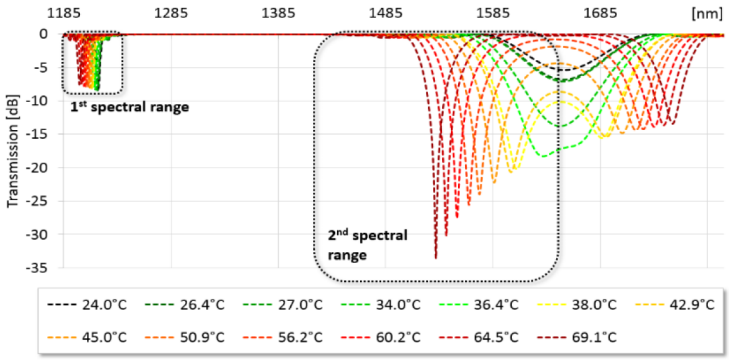

Fig. 7. Simulated transmission spectra versus temperature for the LPFG coated with the 1702 LC layer.

In Fig. 6 and Fig. 7, the measured and the simulated temperature responses of the LPFG are shown. As can be seen, the dual-resonance band starts to generate again in the LC-LPFG transmission when the temperature rises above 32°C, as illustrated in Fig. 5. With a further temperature increase, the central wavelengths of the peaks of the dual-resonance band move in opposite directions. After stabilizing the temperature at the optimal values, we applied an electric field to the sample. In Fig. 8, the simulated transmission spectra for this LC-LPFG in off- and on-voltage states are shown. The spectra were calculated for three different temperatures: 36.4°C, 50.9°C and 60.2°C. Data for the experimentally measured LC-LPFG transmission spectra under the same conditions are shown in Fig. 9(a). As can be seen, in the presence of an E-field the dual-resonance attenuation band disappears. This phenomenon can be explained by two effects that are manifest when the LC-LPFG is heated. First, from the host fiber perspective, the LPFG based on the boron co-doped fiber exhibits a splitting in the dual-resonant attenuation band - see Fig. 1. Second, from the LC layer perspective, the n_e value of the 1702 LC shows an important decrease with an increase in temperature: by 0.053 RI units (RIU) over a temperature cycle range from 32°C to 76°C (for the n_o of 1702 LC this

#255891 Received 16 Dec 2015; revised 18 Feb 2016; accepted 19 Feb 2016; published 4 Mar 2016

change is not so significant and is 0.001 RIU within this same temperature range). Such a variation of the n_e will prevent the recovery of the new attenuation band close to the TAP.

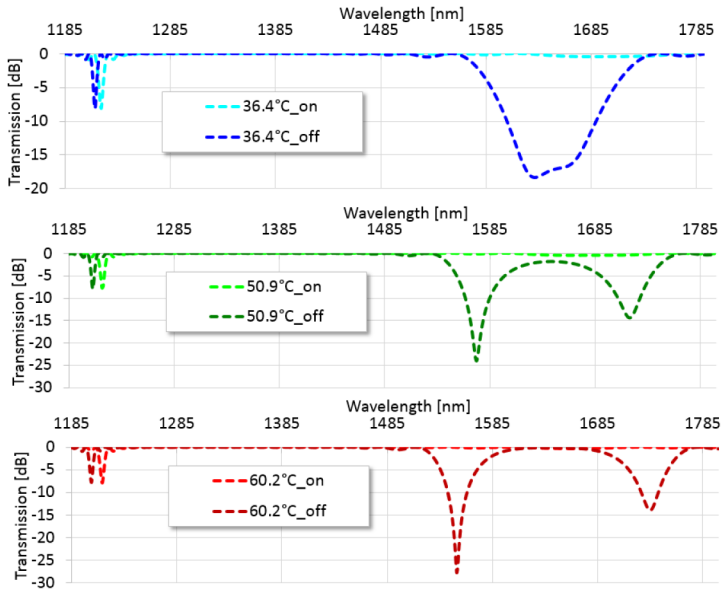

Fig. 8. Simulated transmission in the off- and on-voltage states for the UV-induced LPFG calculated for three different ambient temperature: 36.4°C (a), 50.9 °C (b) and 60.2 °C (c).

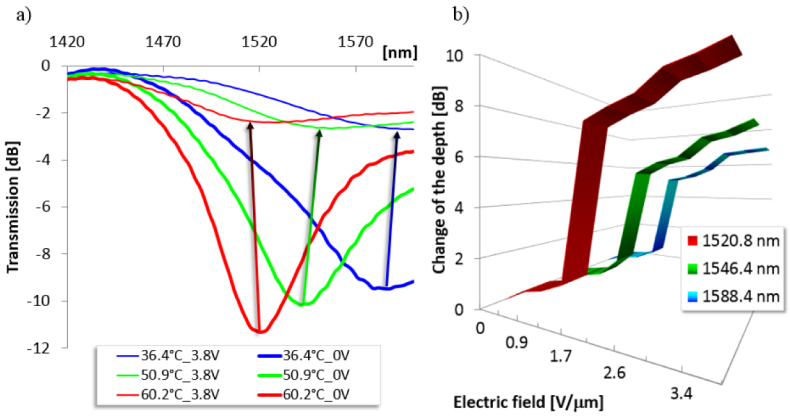

Fig. 9. (a) Transmission spectra in the off- and on-voltage state measured for the LPFG coated with 1702 LC layer when the ambient temperature was stabilized to be 36.4°C, 50.9 °C and 60.2 °C. (b) The attenuation band depth change versus electric field measured for three different values of temperature (36.4°C, 50.9 °C and 60.2 °C) which correspond with three different values of wavelength operation (1520.8 nm, 1564.4 nm and 1588.4 nm).

The above explanation is also confirmed by the way the attenuation band, measured from 1185 nm to 1240 nm, is thermally tuned. Figure 10 gives the thermal responses in the off- and on-voltage states experimentally measured for this attenuation band. As we can see, when the E-field is applied to the sample, a red shift of the resonant wavelength occurs with temperature increase (which is opposite to the resonant wavelength shift measured in the off-voltage state). As a result, the electrical sensitivity of this attenuation band can be controlled efficiently by varying the temperature. Thus, for example, at 25°C the attenuation band is blue-shifted by 8 nm when the E-field is applied to the LC-LPFG, at 30°C the attenuation

#255891 Received 16 Dec 2015; revised 18 Feb 2016; accepted 19 Feb 2016; published 4 Mar 2016

band is insensitive to the E-field presence, and at 50.9°C the attenuation band is red-shifted by 9.5 nm in the on-voltage state.

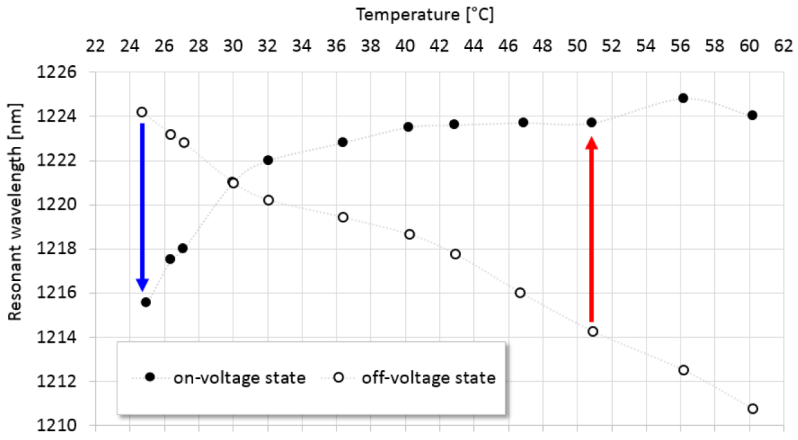

Fig. 10. Thermal sensitivities in on- and off-voltage states for the attenuation band measured in the spectral range from 1185 nm to 1240 nm.

5. Conclusion

The LC-LPFG design proposed here offers extremely interesting properties and useful characteristics, thus introducing a new level of sensitivity and improved performance. The ability of an LPFG to perform as a sensor is highly dependent on the grating period. In this work, a UV-induced host grating with a relatively short period of 226.8 μm was selected. This LPFG design enables coupling of light from the propagating core mode to a cladding mode at a wavelength near the TAP. This phenomenon is exploited here for the first time, to our best knowledge, to measure the thermal and electric field responses of the LC-LPFG structure.

We demonstrated that the attenuation band close to the TAP can be easily altered for particular needs by adjusting the ambient temperature. As shown in Fig. 9(b), the wavelength of operation could be fixed at 1520.8 nm, 1564.4 nm and at 1588.4 nm for a temperature of 36.4°C, 50.9°C and 60.2°C, respectively. When the external E-field was applied to the sample, this attenuation band could be effectively switched on or off. Such high variations in amplitude can be exploited in the same manner as wavelength shift in sensor applications.

We also found that applying the E-field to the LC-LPFG changes the sign and magnitude of the thermal response of the attenuation band measured in the spectral range from 1185 nm to 1240 nm. The electric response of the LC-LPFG could therefore be adjustable over a wide sensitivity range, from an increase in electric sensitivity down to its compensation. Moreover, an electrically induced shift of the attenuation band changes its direction when temperature increases. As shown in Fig. 10, at a temperature range between 25°C and 29°C, the attenuation band is blue-shifted when the E-field is applied to the LC-LPFG; at 30°C, the attenuation band is insensitive to the E-field presence; and within the temperature range from 31°C to 60°C, the attenuation band is red-shifted in the on-voltage state.

To better understand the underlying principles of operation, we developed a model of the thin-layer-coated LC-LPFG. The software tool chosen for modelling was OptiGrating v.4.2. The calculations performed allowed us to qualitatively analyze the LC-LPFG from a theoretical perspective. Our analysis confirmed that the measured attenuation band in the infra-red spectrum comes from coupling of the cladding mode, indicating a dual-resonance phenomenon. The modeling of the LC-LPFG thermal and electric responses provided a good match with the experimental results. We also found that the electrical switching effect in the attenuation bands of the LC-LPFG transmission spectrum occurs thanks to the cladding modes' transition.

#255891 Received 16 Dec 2015; revised 18 Feb 2016; accepted 19 Feb 2016; published 4 Mar 2016

The study presented here will contribute to further development of similar advanced tunable devices that have no counterpart on the current market of active fiber components. The major benefit of these devices is that their spectral properties can be adjusted and controlled with outstanding flexibility. A further benefit is that the optical signal is formed and modified directly in the fiber (all-in-fiber), avoiding a variety of complex alignment issues. Such devices can be easily coupled to optical fibers (useful whenever there is a need for high-performance fiber-optic systems). They can be created with fairly low production costs, since they are based on elements already produced with advanced manufacturing technology and well-developed know-how. From a wider perspective, the work presented here can contribute to the fabrication and practical implementation of LC-LPFG-based photonic devices which can be produced as individual components (including tunable filters, all-in fiber attenuators, threshold sensors, temperature and electric field sensors, switches, and all-optical multi-parameter sensors), or as complements to existing fiber-optic systems. Nevertheless, it has to be added that some challenges still remain to be addressed in the LC-LPFG technology. The coating technique of the fiber surface with a LC is still not finally optimized (nevertheless, the LC layer thickness on the LPFG investigated could be established through the LC-LPFG modeling process). In this work, the rubbing technique was applied. The next possible improvement involves pre-coating of the LPFG with a thin orientation layer for a LC e.g. by using a polyimide resin [22,23]. In addition, many of these materials possess high refractive indices. This could be a supplementary advantage of their use, as it increases the LPFG sensitivity to higher values of the LC refractive indices and may even provide novel tuning effects. New sensing properties could be also obtained by choosing different LCs and/or host LPFGs. In this work, the LCs were applied selectively in the nematic phase. However, the variety of LCs is large. Ferroelectric LCs [24] or lyotropic chromonic LCs for biological sensing application [25, 26], are only a few examples of LC materials that might be used in combination with LPFGs to enhance their tuning properties. It could be also interesting to fabricate a LPFG based on the fiber made of high-index glass. Such a grating would be a very suitable candidate to be combined with a LC, since it could offer higher sensitivities to the values of LC RI, greater than RI of the silica glass. It also has to be added that since two parallel electrodes were used in the presented experimental setup, anisotropy to the LC layer can be induced by an E-field. However, the LC layer is the only portion of the fiber cross section that is birefringent (the core and clad region of the host fiber are supposed to be insensitive to the state of polarization), and is also relatively small compared to the fiber dimensions. Secondly, the LC birefringence affects only the LPFG in terms of its sensitivity to LC layer RI. The pre-tilt of the LC director and/or a geometrical effect resulting from the cylindrical shape of the optical fiber are additional factors, which can also decrease the effect of the LC layer anisotropy. When higher values of birefringence or Polarization Dependent Losses are desirable, the LC-LPFG polarization properties could be well exploited. For this purpose, the LC with high birefringence and dielectric anisotropy would be the best choice. Additionally, in order to achieve LCs molecules' orientation tuning (modified by an E-field), a different electrode configuration could be used, e.g.: multi-electrode system allowing for dynamic change of not only of the E-field, but also its direction [27].

Acknowledgments

This work was supported by the Natural Sciences and Engineering Research Council of Canada and by the Canada Research Chairs Program. The authors are also grateful to the Fonds Québécois de la Recherche sur la Nature et les Technologies (FQRNT).

#255891 Received 16 Dec 2015; revised 18 Feb 2016; accepted 19 Feb 2016; published 4 Mar 2016